Scientific Research Publishing

American Journal of Analytical Chemistry, 2022, 13, 461-475
https://www.scirp.org/journal/ajac
ISSN Online: 2156-8278
ISSN Print: 2156-8251

The Performance Study on Adsorption of SO_2 of CuO Modifying 13X Zeolite Molecular Sieve

Dayi Qian[1,2], Yuebo Zheng[1], Peiliang Shi[2,3*], Wei Su[2], Zhensong Tong[3], Baorui Liang[4], Yan Wang[2]

[1]Key Laboratory of Pollutant Chemistry and Environmental Treatment, School of Chemistry and Environmental Science, Yili Normal University, Yining, China
[2]School of Energy Environmental Engineering, University of Science and Technology Beijing, Beijing, China
[3]BGRIMM Technology Group, Beijing, China
[4]Tianjin College, University of Science and Technology Beijing, Tianjin, China
Email: *peiliang.shi@qq.com

How to cite this paper: Qian, D.Y., Zheng, Y.B., Shi, P.L., Su, W., Tong, Z.S., Liang, B.R. and Wang, Y. (2022) The Performance Study on Adsorption of SO_2 of CuO Modifying 13X Zeolite Molecular Sieve. *American Journal of Analytical Chemistry*, **13**, 461-475.
https://doi.org/10.4236/ajac.2022.1311031

Received: September 21, 2022
Accepted: November 19, 2022
Published: November 22, 2022

Abstract

Research and development of efficient, economical and resource-based flue gas desulfurization technology has always been a hot spot in the field of air pollution control. Molecular sieve materials have been paid attention to by SO_2 adsorbent researchers due to their huge specific surface area. In this paper, 13X zeolite was modified with $Cu(NO_3)_2 \cdot 3H_2O$ to obtain 13x-Xwt %CuO (calculated by the amount of CuO loaded). The adsorption time and capacity of SO_2 penetration sorbent and the isothermal curve of N_2 adsorption-desorption were studied. The results are as follows: 13X-3wt%CuO has the best adsorption effect, the penetration adsorption time is 110 min, the penetration adsorption capacity is 43.41 $mg \cdot g^{-1}$, the saturation adsorption capacity is 49.27 $mg \cdot g^{-1}$; The amount of CuO loading has a great influence on the adsorption effect of modified 13X molecular sieve on SO_2. SEM and BET characterization showed that CuO modification did not change the external morphology of 13X molecular sieve, changed the pore size, but did not block the original channel of the molecular sieve, before and after modification belong to the type I adsorption isothermal curve. The pore size distribution and type of molecular sieve, as well as the content and type of alkali metal cations jointly control the adsorption process of SO_2 by 13X-xwt %CuO. XPS characterization showed that $Cu(NO_3)_2$ decomposed into CuO and Cu_2O during roasting at 450˚C, $CuO/Cu_2O \approx 1.5$. The R^2 values of the quasi-second-order kinetic models obtained from the 13X-Xwt %CuO particle diffusion kinetic models were all above 0.99, indicating that the quasi-second-order kinetic equations were more relevant. Particle diffusion dynamics model in fitting results show that the adsorption process can be divided into two stages, the first phase of surface adsorption and diffusion rate in the granules common control process, more accurate dynamics model of the secondary in the second

phase particle diffusion rate control stage, mainly for the micropore adsorption or chemical adsorption, quasi level 2 dynamic model conformity of variation; C is a constant not equal to 0, indicating that the adsorption of SO_2 is not completely through the form of intra-particle diffusion, and a small amount of chemisorption exists. And it is the compound effect of multiple adsorption mechanisms.

Keywords

Air Pollution Control, Zeolite Molecular Sieve, Adsorbent, Flue Gas Purification, Sulfur Dioxide

1. Introduction

There are many mature methods to purify SO_2 in flue gas, which only realize the transmedium transfer of pollutants and have a large amount of CO_2 emission. Dry adsorption desulfurization technology can effectively recover SO_2 and realize resource utilization, which has become one of the most potential treatment approaches. Common SO_2 adsorbents include activated carbon, silica gel, zeolite molecular sieve, metal-organic frame materials, etc. Activated carbon and molecular sieve are the most widely used adsorbents at present, but the cost becomes high and it is easy to ignite, which puts forward higher requirements for operation and maintenance [1] [2]. Therefore, it is urgent to develop a kind of adsorbent with high efficiency, low cost, strong thermal stability and large adsorption capacity.

Molecular sieve is a kind of homogeneous micropore, which has great application potential in the field of SO_2 adsorption and removal. However, molecular sieve has high regeneration temperature, water sensitivity and other shortcomings, become the bottleneck of zeolite desulfurization application. Studies have shown that pore structure and modification methods become the key factors to improve the reactivity, prolong the service time and improve the adsorption performance [3] [4] [5]. H. Taghdisian *et al.* [6] found that the Coulomb interaction between cations in 5A and 13X and diffused SO_2 could reduce the mobility of SO_2. The passage of zeolite molecular sieve contains a large number of alkali metal cations, through certain modification means, can change the content of alkali metal cations in the passage. Yunrong Dai *et al.* [7] believe that the adsorption performance of molecular sieve for pollutants is closely related to the flexible crystal structure of molecular sieve and the respiratory vibration of its pore. Xiaoshan Li *et al.* [8] also showed that the absorption rate of SO_2 depends on the pore size distribution of molecular sieve. The characteristics of molecular sieve in addition to the specificity of the structure and the variety of diversification, and their structure and performance of the modifiable also have a close relationship. Dealuminization modification and desilication modification can not only make the molecular sieve form a large number of multistage pores, but also

prolong its life. Compared with dealuminization and desilication modification, metal modification can effectively improve the yield and selectivity of target products, improve the adsorption/catalytic activity of molecular sieve, prolong its life, and avoid the corrosion of acid and alkali, which is safer. Yang Yuhui *et al.* [9] found that K^+, Mg^{2+} and Ca^{2+} could improve the L-acid content and reducibility of AgY, thereby enhancing its sulfur adsorption performance. K. Yang *et al.* [10] used 13X as the adsorbent to remove H_2S and SO_2 at the same time. The research results showed that the sulfur penetration capacity of 13X could reach 179.7 mg/g, 3 times that of activated carbon (64.3 mg/g), and the regeneration performance was good, and the service life of molecular sieve was prolonged. Amvrosios G *et al.* [11] studied the desulfurization performance of zeolite molecular sieve, and discussed the influence of temperature, inlet concentration, gas matrix and regeneration cycle times on the desulfurization performance of IMS. After 15 adsorption/desorption cycles, IMS could be completely regenerated. Thermodynamic studies confirmed that physical adsorption was dominant.

In this study, CuO is used to modify 13X molecular sieve, and 13X molecular sieve adsorbent with high adsorption capacity is prepared. Through the characterization of material properties, the influence of CuO load and adsorption reaction temperature on the adsorption effect of SO_2, the study of particle diffusion kinetics and internal diffusion kinetics model fitting on the adsorption mechanism, lay a technical and theoretical foundation for its practical application.

2. Experimental Materials and Methods

2.1. Material

In the early stage, through screening three kinds of zeolite molecular sieves (4A, 5A, 13X) commonly used in industry, the best adsorbent 13X molecular sieves were selected. 13X molecular sieve samples were purchased from Sinopharm chemical reagent Co., LTD. (≥99.0%), molecular formula: Mx/m $[(AlO_2)_x(SiO_2)_y]_zH_2O$. All the other reagents were also purchased from Sinoprecipent Chemical Reagent Co., LTD except sodium hydroxide (Beijing Chemical Reagent Company) and potassium bromide (Belgium Acros). N_2 (99.999%, Beijing Praxair Practical Gas Co., LTD.), O_2 (99.999%, Beijing Zhaoge Gas Co., LTD.) and SO_2/N_2 (1%, Beijing Zhaoge Gas Co., LTD.).

2.2. Experimental Methods and Procedures

A certain quantity of $Cu(NO_3)_2{\cdot}3H_2O$(calculated by the amount of CuO loaded) was added to 20 mL deionized water to completely dissolve it. The beaker containing the solution was placed on a constant temperature magnetic stirrer, and the constant temperature magnetic stirrer was adjusted to 40˚C. A certain amount of molecular sieve was weighed and slowly added into the copper nitrate solution in the stirring process. After 1 h, the beaker was removed. After 12 h, the sample was placed in a centrifuge at 500 R/min to eliminate the interference of excess Cu^{2+}. The prepared samples then were dried in an oven at 150˚C and roasted in Muffle furnace at 450˚C for two hours. Finally, CuO modified 13X

molecular sieve modified adsorption material was obtained, hereinafter referred to as 13X-xwt%CuO (mass fraction of X-loaded CuO). The modified materials were characterized by scanning electron microscopy (SEM), specific surface area and pore structure (BET), X-ray photoelectron spectroscopy (XPS) and X-ray diffraction (XRD).

Referring to the composition of industrial flue gas, the main gas components except dust were simulated in the laboratory. The main components of the simulated flue gas are SO_2, N_2, O_2, H_2O(g), and the four gas components (volume fraction) are set as follows: 0.3%, 83.7%, 6%, 10%. The total volume flow of simulated flue gas was 500 mL·min^{-1}, the temperature was 110˚C (actual outlet temperature of industrial flue gas), and the space speed (GHSV) was 1200 h^{-1}. The experimental setup was shown in Figure 1.

The accurately weighed modified adsorbent was loaded into the experimental device, and the pollutant gas was injected into the experimental device after the investigation conditions were preset. The exhaust gas components after passing through the adsorption bed are detected to investigate the adsorption situation of the bed. The exhaust gas components after passing through the adsorption bed are detected, and the saturation desulfurization value and penetration desulfurization value are taken as the evaluation indexes to investigate the adsorption situation of the bed. Sulfur capacity saturation value is the maximum adsorption mass of unit mass modified zeolite molecular sieve for SO_2.

This experimental study is to use CuO modified zeolite molecular sieve to adsorb SO_2 gas, so that it can meet the national emission standard-GB-13271-2014 boiler air pollutants emission standard. Therefore, the penetration point of SO_2 in the outlet gas is positioned at 200 ppm. In the analysis of experimental data, when the outlet SO_2 reaches the specified penetration point, the adsorption capacity of the adsorbent is used as the basis for evaluating the activity of the desulfurizer. The calculation formula of the penetration adsorption capacity is as follows:

$$q = \frac{10^{-6} Q \int_0^{t_m} \left(C_0 - C_1 \right) dt}{22.4G} \tag{1}$$

where q is the adsorption capacity of the adsorbent when the outlet SO_2 reaches the adsorption penetration point, mmol·g^{-1}; G is the adsorbent mass, g; t is the time for outlet SO_2 to reach the penetration point, min; C_0 is the Concentration of SO_2 at the air inlet, ppm; C_1 is the Concentration of SO_2 at the air outlet, ppm; Q is the Total gas flow, mL·min^{-1}.

2.3. Analysis and Testing Instrument

Main equipment: Electronic balance (ML-104, Mettler-Toledu), Fourier transform infrared spectrometer (IS50, ThermoFisher), SO_2 analyzer (CLD62, Switzerland Eco Physics), Automatic surface area and aperture distribution analyzer (AutoSORB-IQ, Quantachrome), XPS (250XI, Thermo Fisher), XRD (Smartlab9kw, Rigaku) gas distribution system and related accessories.

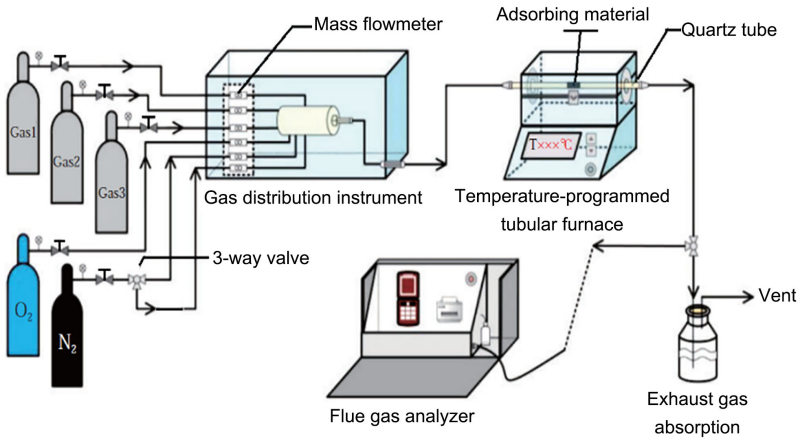

Figure 1. Experimental device for adsorption of SO_2 by zeolite molecular sieve.

2.4. Study on Adsorption Kinetics

The study of adsorption kinetics can not only estimate the kinetic adsorption rate of molecular sieve, but also speculate the adsorption mechanism. Some experts and scholars have analyzed the fluid structure and dynamics of different types of adsorbent materials, and discussed the kinetic diffusion behavior of adsorbent in adsorbent, as well as the diffusion and migration mechanism of gas in molecular sieve. In this experiment, the quasi-first-order and quasi-second-order kinetic models and the intra particle diffusion model equations were used to fit the SO_2 adsorption data of modified 13X-xwt%CuO molecular sieve, so as to analyze the removal mechanism of SO_2 by modified materials.

1) Fitting analysis of quasi-first-order and quasi-second-order adsorption kinetics models

Equation of quasi-first-order dynamic model [12]:

$$\ln\left(q_e - q_t\right) = \ln q_e - k_1 t \tag{2}$$

where q_e is the equilibrium adsorption capacity of SO_2, $mg \cdot g^{-1}$; q_t is the adsorption capacity at reaction time t, $mg \cdot g^{-1}$; k_1 is the quasi-first-order adsorption rate constant, min^{-1}.

The quasi-second-order adsorption kinetic model is established on the basis of Langmuir isothermal adsorption equation, which is commonly used to describe the chemisorption process with ion migration. If the adsorption process involves the formation of new chemical bonds, the adsorbent will be firmly bound to the surface of the adsorbent due to the role of chemical bonds. This model assumes that the adsorption rate in the adsorption process is linearly squared with the remaining adsorption active sites in the absorbent. Therefore, the quasi-second-order adsorption kinetic model can be expressed by the following equation [13]:

$$\frac{dq_t}{dt} = k_2\left(q_e - q_t\right)^2 \tag{3}$$

After integration, we can get:

$$q_t = \frac{k_2 q_e^2 t}{1 + k_2 q_e t} \tag{4}$$

where q_e is the equilibrium adsorption capacity of SO_2, mg·g^{-1}; q_t is the adsorption capacity at reaction time t, mg·g^{-1}; k_2 is the Quasi-second-order adsorption rate constant g·(mg·min)$^{-1}$.

2) Model equation for intra-particle diffusion

The kinetic model could not elucidate the diffusion mechanism and rate control steps of SO_2 adsorption on molecular sieve. Therefore, the Weber-Morris particle diffusion model was selected, which was proposed by Weber-Morris *et al.* on the basis of Fick's second diffusion law. The model is mainly used to describe the adsorption process dominated by diffusion in pores, and the adsorption process can be analyzed according to the internal diffusion rate constant. If the fitted curve is linear with $T^{0.5}$, it indicates that particle diffusion is a way to adsorb SO_2. If the fitted curve with $T^{0.5}$ passes through the origin, it indicates that intra-particle diffusion is the only way for molecular sieve to adsorb SO_2. The adsorption rate equation of the intra-particle diffusion model is as follows [14]:

$$\frac{dq_t}{dt} = 0.5 k_1 t^{-0.5} \tag{5}$$

when $t = 0$, $q_t = 0$; When $t = t$, $q_t = q_t$; After integration, we can get:

$$q_t = k_1 t^{0.5} + C \tag{6}$$

where q_t is the Adsorption capacity of unit mass adsorbent for SO_2 at time t, mg·g^{-1}; k_1 is the internal diffusion rate constant, mg·g^{-1}·min$^{-0.5}$; C is the intercept, boundary layer thickness, mg·g^{-1}; T is the Reaction time, min.

3. Experimental Results and Discussion

3.1. Adsorption of SO_2 by 13x-X %wtCuO Molecular Sieve

The adsorption and penetration curves of 13X zeolite supported with different mass fractions of CuO are shown in **Figure 2**.

As can be seen from **Figure 2**, the time for 13X zeolite with different CuO loads to completely adsorb SO_2 from large to small is: 13X-3%WTCuO > blank sample > 13X-6%WTCuO > 13X-9%WTCuO, indicating that CuO, as an active component, can improve the adsorption capacity of SO_2 by zeolite in a certain range of loading capacity, and the penetration adsorption capacities are 37.55 mg·g^{-1}, 43.41 mg·g^{-1}, 35.19 mg·g^{-1} and 22.53 mg·g^{-1}, respectively. The saturated adsorption capacities were 41.14 mg·g^{-1}, 49.27 mg·g^{-1}, 42.95 mg·g^{-1} and 30.21 mg·g^{-1}, respectively. The amount of CuO loading had a great influence on the adsorption effect of modified 13X molecular sieve. It may be that the addition of CuO changes the specific surface area of molecular sieve, changes the pore structure, and increases the porosity. Cu^{2+} enters the pore and enhances the Coulomb force between molecules. At the adsorption temperature of 110˚C, physical adsorption dominates, and the conditions for chemisorption are insufficient.

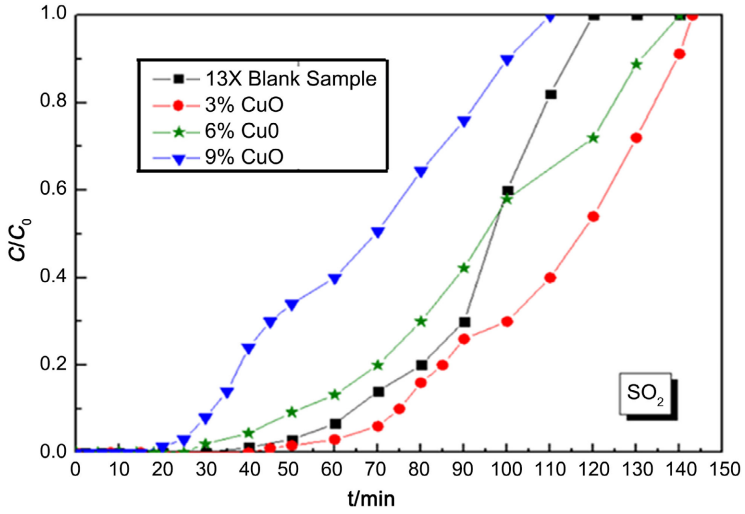

Figure 2. Adsorption and penetration curves of 13X molecular sieve with different CuO loading.

Studies have shown that [7]: The richer the pore structure of the adsorption material, the larger the specific surface area, and the surface can provide a large number of adsorption active sites, which means that the adsorption capacity is higher. In this study, by means of CuO modification, the content and type of alkali metal cations in the pores of 13X molecular sieve were changed, and part of the crystal water in the pores was removed by roasting at high temperature, so as to change the pore size and type of zeolite and the pore size distribution and type of molecular sieve. And the content and type of alkali metal cations jointly control the adsorption process of SO_2 by 13x-xwt %CuO.

3.2. SEM Characterization Analysis

The adsorption effect of SO_2 by molecular sieve is related to the pore size and specific surface area of molecular sieve itself.

Figure 3 shows the comparison of SEM characterization of 13X molecular sieve blank sample, 13X-3%CuO and 13X-9%CuO. As can be seen the surface of 13X molecular sieve has bulges or depressions of different shapes and sizes distributed irregularly on the surface of the material, increasing the specific surface area of the material. The morphology of 13X-3%CuO (10 μm) and 13X-9%CuO (5 μm) is not significantly changed from that of 13X blank sample (10 μm).

3.3. BET Characterization Analysis

Figure 4 shows the N_2 adsorption-desorption curve of loaded 3wt%Cuo-13x and blank sample. **Figure 5** shows the pore size distribution diagram of loaded 13x-3wt%CuO and blank sample.

It can be seen from **Figure 4** that the adsorption isotherms of 13X zeolite and 13X blank samples after CuO loading belong to type I adsorption isotherms. The characteristic is that when the relative pressure is very small, the curve shows a

significant rise, and then the curve remains basically stable. This is also a characteristic of typical microporous materials. When P/P0 is 0.8, 13x-3wt %CuO shows insignificant hysteresis loop, which may be due to capillary agglutination in the molecular sieve. This phenomenon generally occurs in mesoporous pores, which indirectly proves that the load distribution of 3wt%CuO on 13X molecular sieve is relatively good and does not block the original pore of molecular sieve.

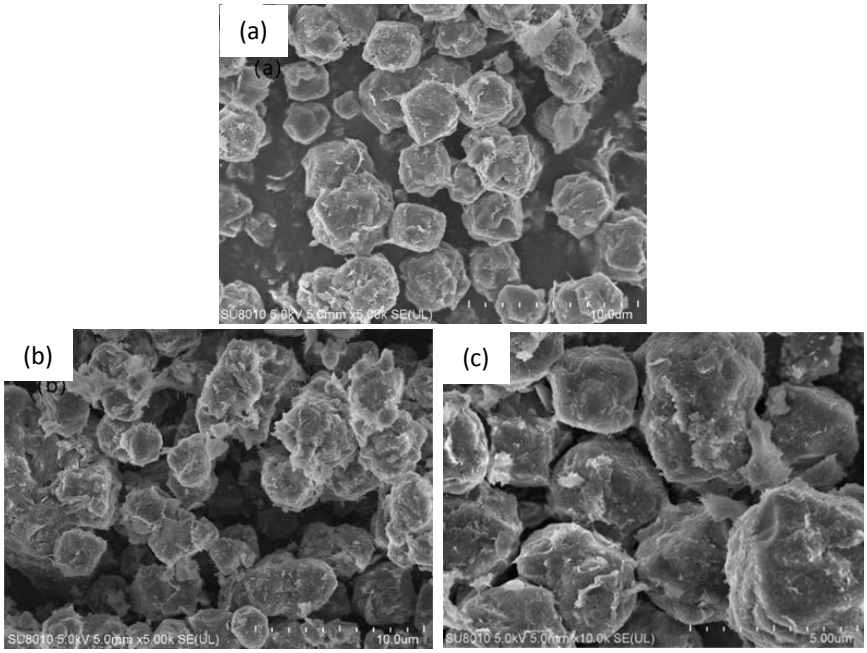

Figure 3. SEM comparison of 13X-xwt%CuO molecular sieve before and after modification. (a) 13X Blank Ample (10 μm); (b) 13X-3wt%CuO (10 μm); (c) 13X-9wt%CuO (5 μm).

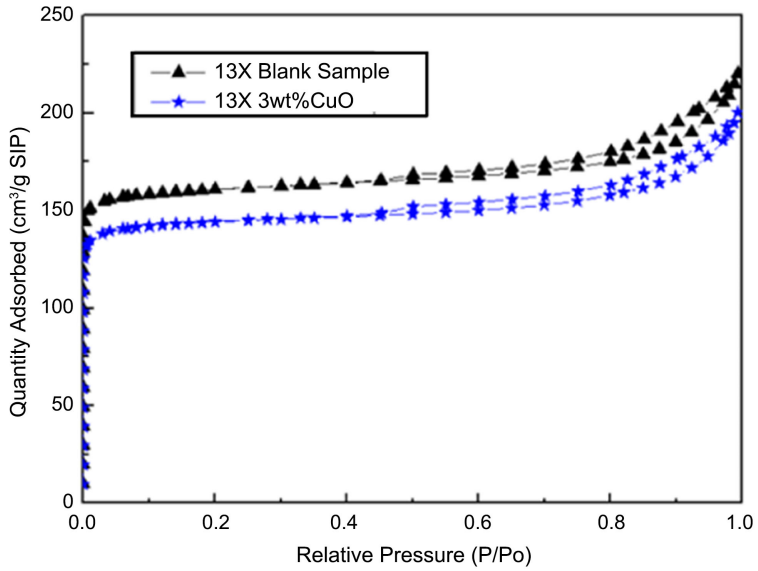

Figure 4. N_2 adsorption-desorption curve of 3wt%CuO-13X and 13X.

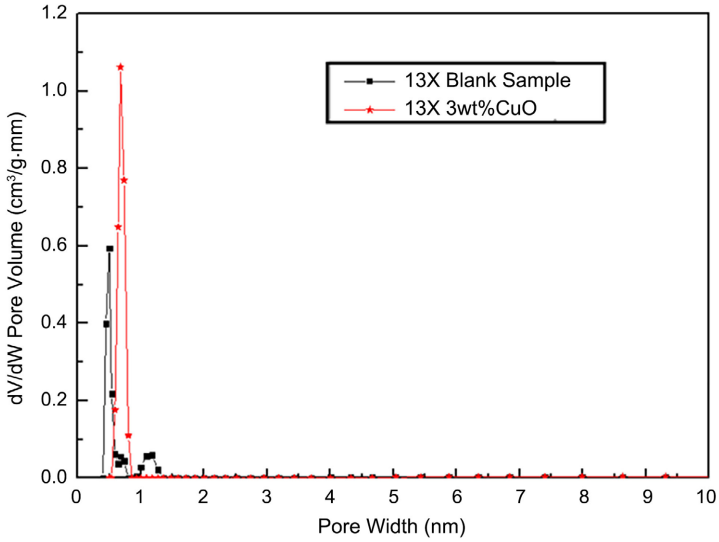

Figure 5. Pore size distribution of 3wt%CuO-13X and 13X.

Combined with **Figure 5**, it can be seen that after the modification of 13X molecular sieve by CuO active component, the pore size distribution map becomes a symmetric peak. Compared with the untreated 13X molecular sieve, the pore size distribution is slightly changed, from the original two peak distribution concentrated between 0.4 - 0.8 nm and 1.0 - 1.3 nm to the uniform distribution between 0.5 - 0.9 nm. This indicates that the addition of CuO can change the original pore size of molecular sieve. In the process of CuO modification of 13X zeolite, the addition of $Cu(NO_3)_2{\cdot}3H_2O$ and the dissolution of NO_3^- and roasting at 450˚C for a long time resulted in the increase of the small pore size and the disappearance of the large pore size.

The area enclosed by the 13x-3wt %CuO curve is significantly larger than that of the blank sample, indicating that the pore volume increases, which proves that CuO does not block the pore.

3.4. XPS Energy Spectrum Analysis

Figure 5 shows the XPS map of 13X-3wt%CuO, so as to obtain the loading situation of CuO on 13X molecular sieve and the valence state of Cu element. $Cu(NO_3)_2$ decomposed into CuO and Cu_2O or both after roasting at high temperature. All elements except H and He are identified according to the positions of the characteristic spectral lines in the energy spectra measured by XPS. The content or relative concentration of reactive atoms can be obtained from the intensity of the photoelectron line (the area of the photoelectron peak) in the XPS energy spectrum.

According to the XPS total spectrum in **Figure 6**, the characteristic peaks of copper ions appeared on the surface of the modified 13X molecular sieve, which proved the existence of Cu ions. In order to further show that CuO is successfully loaded after 13X modification, the XPS map of Cu element is analyzed as follows: **Figure 7** peak fitting is performed using the Gaussian/Laurentus equa-

tion minimum mean square error Shirley elimination method. It can be seen that it is composed of two peaks, which are CuO and Cu_2O peaks respectively. This indicates that CuO and Cu_2O are generated by $Cu(NO_3)_2$ decomposition at 450˚C. By comparing the area of CuO and Cu_2O peaks, $CuO/Cu_2O \approx 1.5$ can be obtained. This indicates that $Cu(NO_3)_2$ is not completely transformed into CuO after roasting at 450˚C for 2 h.

3.5. Study on Adsorption Kinetics

1) Adsorption kinetic model fitting analysis

Figure 8 shows the fitting curves of CuO modified 13X-Xwt %CuO molecular sieve adsorption materials when the adsorption performance of SO_2 reaches the penetration point for quasi-first-level (a) and quasi-second-level (b) adsorption kinetic models. Table 1 shows the relevant fitting parameters and determination coefficient R^2.

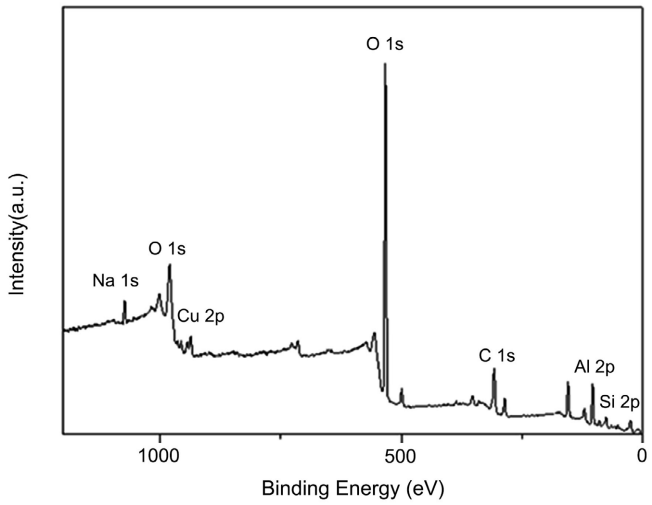

Figure 6. XPS pattern of 13X-3wt% CuO.

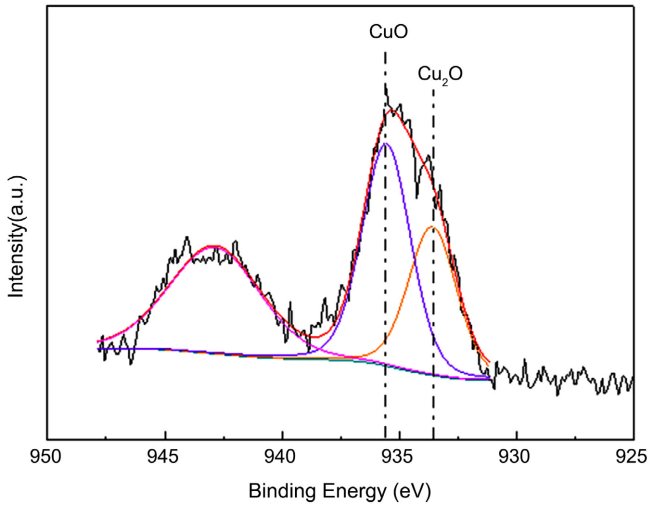

Figure 7. XPS pattern of Cu element.

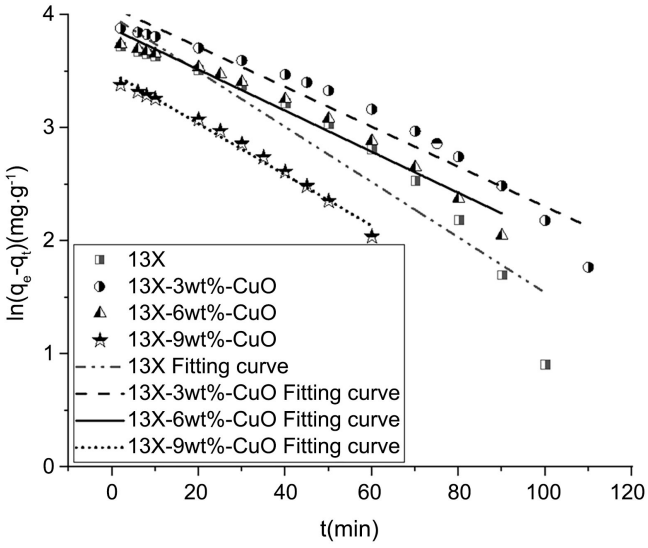

(a)

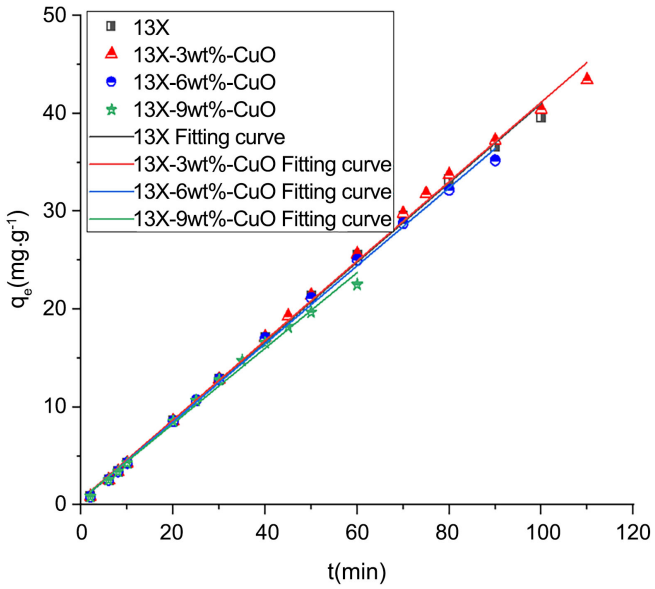

(a)

Figure 8. Fitting curve of adsorption kinetics model. (a) Quasi first order model; (b) Quasi second-order model.

Table 1. Fitting parameters and determination coefficients of adsorption kinetics model.

Adsorbent	Through the time *t*/min	Quasi first order model		Quasi second-order model	
		k_1/min^{-1}	R^2	k_2/g·mg^{-1}·min^{-1}	R^2
13X	95	−0.9543	0.9108	0.4053	0.9982
13x-3wt%CuO	110	−0.9742	0.9490	0.4055	0.9976
13x-6wt%CuO	90	−0.9857	0.9716	0.3984	0.9980
13x-9wt%CuO	60	−0.9942	0.9884	0.3856	0.9943

It can be seen intuitively from Figure 8 that the quasi-second-order curve is basically a straight line, and the quasi-first-order curve approximately presents a free-fall curve with the increase of adsorption time. As can be seen in Table 1, the R^2 values of the quasi-first-order kinetic model are all smaller than those of the quasi-second-order kinetic model, and the R^2 values of the quasi-second-order kinetic model are all above 0.99 and close to 1, indicating that the quasi-second-order kinetic equation is more relevant and can better describe the adsorption process of SO_2 by CuO modified 13X-Xwt %CuO molecular sieve adsorption material. When the adsorption capacity of SO_2 exceeds a certain amount, the correlation of the quasi-second-order kinetic model becomes worse, indicating that the adsorption process of SO_2 by 13x-xwt %CuO is controlled by multiple factors.

2) Kinetic model fitting analysis of diffusion in particles

The kinetic model could not fully elucidate the diffusion mechanism and rate control steps of 13x-xwt%CuO for SO_2 adsorption. Therefore, the adsorption process of adsorbent on adsorbent is often described by Weber-Morris particle diffusion model.

Figure 9 and Table 2 show the results after fitting the kinetic model of diffusion in 13X-Xwt %CuO particles. The results show that QT and $T^{0.5}$ show broken lines, indicating that diffusion in particles is not the main control step of the rate. The adsorption process can be roughly divided into two stages: the first stage (from the beginning of air intake to the penetration point) is the rapid adsorption stage, which is characterized by the joint control process of surface adsorption and intra-particle diffusion rate, and the adsorption contribution rate is large, accounting for about 90%. This stage is also more consistent with the quasi-second-order adsorption kinetic model. The second stage (from the penetration point to adsorption saturation) is the control stage of the diffusion rate in particles, which is mainly microporous adsorption or chemisorption. The adsorption amount is small, and is positively correlated with the CuO attachment load, indicating that CuO modification of 13X modified molecular sieve adsorption material enhances the chemisorption performance of molecular sieve, and reduces the physical adsorption performance. At this stage, the correlation of quasi-second-order adsorption kinetics model becomes worse.

Table 2. Fitting parameters and determination coefficients of intra-particle diffusion dynamics model.

Adsorbent	The first stage				The second stage			
	k_1 $mg \cdot g^{-1} \cdot min^{-0.5}$	C $mg \cdot g^{-1}$	R^2	The adsorption quantity %	k_1 $mg \cdot g^{-1} \cdot min^{-0.5}$	C $mg \cdot g^{-1}$	R^2	The adsorption quantity %
13X Blank Ample	0.1499	0.8756	0.9872	90.79	0.0575	8.6812	0.9298	9.21
13x-3wt%CuO	0.1506	0.9479	0.9914	90.01	0.0464	12.252	0.9762	9.99
13x-6wt%CuO	0.1390	0.9870	0.9868	85.81	0.0420	9.2334	0.9609	14.19
13x-9wt%CuO	0.1659	0.4692	0.9879	80.01	0.0487	7.0641	0.9388	19.99

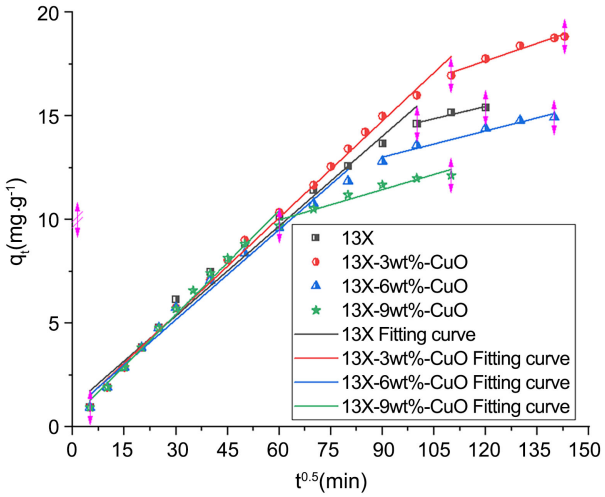

Figure 9. Model fitting curve of diffusion dynamics in particles.

The fitting coefficient of determination R^2 of the two stages is above 0.90, and the R^2 of the first stage is greater than or close to 0.99. The results indicate that the diffusion kinetic model can better explain the adsorption process of SO_2 by modified molecular sieve. Since C in the formula is a constant that is not 0, the curve does not reach the origin, indicating that the removal of SO_2 is not completely adsorbed by the form of intra-particle diffusion, and a small amount of SO_2 is adsorbed by the modified molecular sieve by chemical adsorption. The internal diffusion rate constant k_1 is basically the same, indicating that CuO modification has little effect on the pore size distribution of 13x molecular sieve.

Combined with **Figure 2**, it can be concluded that the modification of 13X molecular sieve with CuO can improve the adsorption performance of the material for SO_2 when the CuO attachment load is about 3%. With the increase of the attachment load, the adsorption performance of the material for SO_2 decreases, but the chemical adsorption amount increases.

4. Conclusions

1) CuO modifies 13X molecular sieve and CuO load has a certain impact on the adsorption of SO_2 modified molecular sieve, adsorption capacity from large to small: 13X-3%wtCuO > blank sample > 13X-6%wtCuO > 13X-9%wtCuO. The best effect is 13X-3wt%CuO, the penetration adsorption time is 110 min, the penetration adsorption capacity is 43.41 mg·g^{-1}, the saturation adsorption capacity is 49.27 mg·g^{-1}. The pore size distribution and type of molecular sieve, as well as the content and type of alkali metal cations jointly control the adsorption process of SO_2 by 13X-xwt %CuO.

2) SEM characterization showed that there was no significant change in the appearance of molecular sieve after CuO modification of 13X-xwt %CuO; BET characterization shows that the adsorption isotherms of 13X zeolite and 13X blank samples after CuO loading belong to type I adsorption isotherms. Compared with the untreated 13X molecular sieve, the pore size distribution changed

slightly, from the original two peak distribution concentrated between 0.4 - 0.8 nm and 1.0 - 1.3 nm to uniform distribution between 0.5 - 0.9 nm, indicating that the addition of CuO can change the original pore size of molecular sieve. The addition of $Cu(NO_3)_2{\cdot}3H_2O$ and the dissolution of NO_3^- and roasting at 450˚C for a long time make the small pore size larger, and the large pore size disappears and no longer becomes a micropore structure. The area enclosed by 13X-3wt%CuO curve is obviously larger than that of blank sample, and the pore volume increases, which proves that CuO does not block the pore. XPS characterization showed that $Cu(NO_3)_2{\cdot}3H_2O$ did not completely decompose into CuO during roasting at 450˚C, but partially decomposed into Cu_2O, $CuO/Cu_2O \approx 1.5$.

3) The R^2 values of the quasi-first-order kinetic model are all less than that of the quasi-second-order kinetic model. The R^2 values of the quasi-second-order kinetic model are all above 0.99, which indicates that the quasi-second-order kinetic equation is more relevant and expresses the composite effect of multiple adsorption mechanisms. The fitting results of the kinetic model show that the diffusion in particles is not the main control step of the rate, and the adsorption process can be divided into two stages: In the first stage, the surface adsorption and the diffusion rate in particles are controlled jointly, and the contribution rate of adsorption is relatively large, which is more consistent with the quasi-second-order adsorption kinetic model. In the second stage, the diffusion rate in particles is controlled, mainly by microporous adsorption or chemisorption, and the adsorption amount is small. In this stage, the correlation of quasi-second-order adsorption kinetic model becomes worse. In the first stage, the fitting coefficient of determination R^2 is about 0.99, indicating that the kinetic model of intra-particle diffusion can better explain the adsorption process of SO_2 by modified molecular sieve. Since C is a constant of non-0, it indicates that the removal of SO_2 is not completely adsorbed by the form of intra-particle diffusion, and there is a small amount of chemical adsorption. The CuO modification of 13X molecular sieve can improve the adsorption performance of the material for SO_2 when the CuO attachment load is about 3%. With the increase of the attachment load, the adsorption performance of the material for SO_2 decreases, but the chemical adsorption increases.

Acknowledgements

Xinjiang Natural Science Foundation project (2022D01C333).

Conflicts of Interest

The authors declare no conflicts of interest regarding the publication of this paper.

References

[1] Feng, Y.C., Yu, Q.J., Yi, H.H., *et al.* (2020) Research Progress of MFI-Type Zeolites in the Field of VOCs Removal. *Materials Reports*, **34**, 17089-17098.

[2] Huang, X.X., Chen, L., Li, H., *et al.* (2020) Research Progress of Activated Carbon Fiber in Flue Gas Desulfurization and Denitrification. *Hongshui River*, **39**, 35-38.

[3] Wang, C.-R. (2010) Study on Performance and Application of Zeolite Molecular Sieve. *Chemistry and Adhesion*, **32**, 76-78.

[4] Soontornworajit, B., Wannatong, L., Hiamtup, P., *et al.* (2007) Induced Interaction between Polypyrrole and SO_2 via Molecular Sieve 13X. *Materials Science & Engineering B*, **136**, 78-86. https://doi.org/10.1016/j.mseb.2006.09.016

[5] Zhang, Y., Chen, Z.H., Liu, X., *et al.* (2020) Efficient SO_2 Removal Using a Microporous Metal-Organic Framework with Molecular Sieving Effect. *Industrial & Engineering Chemistry Research*, **59**, 874-882. https://doi.org/10.1021/acs.iecr.9b06040

[6] Taghdisian, H., Tasharrofi, S., Firoozjaie, A.G., *et al.* (2019) Loading-Dependent Diffusion of SO_2 in 13X and 5A Using Molecular Dynamics: Effects of Extraframework Ions and Topology. *Journal of Chemical & Engineering Data*, **64**, 3092-3104. https://doi.org/10.1021/acs.jced.9b00204

[7] Dai, Y.R., Yin, L.F., Wang, S.Y., *et al.* (2020) Shape-Selective Adsorption Mechanism of CS-Z1 Microporous Molecular Sieve for Organic Pollutants. *Journal of Hazardous Materials*, **392**, Article ID: 122314. https://doi.org/10.1016/j.jhazmat.2020.122314

[8] Li, X.S., Zhang, L.Q., Zheng, Y., *et al.* (2015) SO_2 Absorption Performance Enhancement by Ionic Liquid Supported on Mesoporous Molecular Sieve. *Energy & Fuels*, **29**, 942-953. https://doi.org/10.1021/ef5022285

[9] Yang, Y.H., Liu, M., Song, C.-S., *et al.* (2008) Pereformance of Adsorptive Desulfurization over Modified Y Zeolites. *Acta Petrolei Sinica*, **4**, 383-387.

[10] Yang, K., Su, B.H., Shi, L., *et al.* (2018) Adsorption Mechanism and Regeneration Performance of 13X for H_2S and SO_2. *Energy Fuels*, **32**, 12742-12749. https://doi.org/10.1021/acs.energyfuels.8b02978

[11] Georgiadis, A.G., Charisiou, N.D., Gaber, S., *et al.* (2021) Adsorption of Hydrogen Sulfide at Low Temperatures Using an Industrial Molecular Sieve: An Experimental and Theoretical Study. *ACS Omega*, **6**, 14774-14787. https://doi.org/10.1021/acsomega.0c06157

[12] Thinakaran, N., Baskaralingam, P., Pulikesi, M., *et al.* (2008) Removal of Acid Violet 17 from Aqueous Solutions by Adsorption onto Activated Carbon Prepared from Sunflower Seed Hull. *Journal of Hazardous Materials*, **151**, 316-322. https://doi.org/10.1016/j.jhazmat.2007.05.076

[13] Ho, Y.S. and Mckay, G. (1999) Pseudo-Second Order Model for Sorption Processes. *Process Biochemistry*, **34**, 451-465. https://doi.org/10.1016/S0032-9592(98)00112-5

[14] Chin, W.F., Ling, T.R., Shin, J.R., *et al.* (2009) Initial Behavior of Intraparticle Diffusion Model Used in the Description of Adsorption Kinetics. *Chemical Engineering Journal*, **153**, 1-8. https://doi.org/10.1016/j.cej.2009.04.042